ISSN 0022-4766, Journal of Structural Chemistry, 2021, Vol. 62, No. 11, pp. 1667-1677. © Pleiades Publishing, Ltd., 2021.
Russian Text © The Author(s), 2021, published in Zhurnal Strukturnoi Khimii, 2021, Vol. 62, No. 11, pp. 1780-1790.

SYNTHESIS, CRYSTAL STRUCTURES, AND UREASE INHIBITORY ACTIVITY OF SCHIFF BASE COPPER AND NICKEL COMPLEXES*

Y. Wang**

Urease inhibitors can inhibit the decomposition rate of urea, and decrease the air pollution caused by ammonia. In this paper, three new copper(II) and nickel(II) complexes $[Cu_2L_2(\mu_{1,1}\text{-}N_3)_2]$ (**1**), $[Cu(HL)_2]Br_2$ (**2**), and $[Ni_3L_2(DMF)_2(\mu_2\text{–}\eta^1\text{:}\eta^1\text{-}CH_3COO)_2(\mu_{1,1}\text{-}N_3)_2]$ (**3**), where L = 5-bromo-2-(((2-isopropylamino) ethyl)imino)methyl)phenolate, HL = 5-bromo-2-(((2-isopropylammonio)ethyl)imino)methyl)phenolate are synthesized and characterized. The complexes are characterized by elemental analyses, IR, UV-Vis spectra, molar conductivity, and single crystal X-ray diffraction. The X-ray analysis indicates that Cu atoms in complexes **1** and **2** are in square pyramidal and square planar coordination, respectively. The Ni atoms in complex **3** are in octahedral coordination. The molecules of the complexes are linked through hydrogen bonds and π···π interactions. The inhibitory effects of the complexes on jack bean urease are studied, which show that the copper complexes have a strong inhibitory effect on urease.

DOI: 10.1134/S0022476621110020

Keywords: Schiff base, copper complex, nickel complex, X-ray diffraction, urease inhibitory activity.

INTRODUCTION

Urea is a major nitrogen-containing soil fertilizer, with an annual production projected to reach 226 million tons in 2021 [1]. Once deposited in soil, urea quickly hydrolyzes by urease to yield NH_3 [2]. This reaction causes a number of agronomic, environmental and economic problems and affects the global nitrogen cycle [3-5]. In particular, a too rapid increase in soil pH upon urea hydrolysis catalyzed by the urease activity causes the loss of urea nitrogen as gaseous ammonia which is toxic to plants and contributes to the production of fine inorganic particulate matter [6, 7]. This process causes the tropospheric pollution by NO, NO_2, and N_2O, which is a greenhouse gas with 300 times the heat trapping capacity of CO_2 [8]. Urease occurs widely in most bacteria, plants, algae, fungi, and invertebrates [9, 10]. The urease enzyme catalyzes the highly efficient decomposition of urea into ammonia with a rate 10^{14} times faster than that of the non-catalyzed reaction [11]. This process is harmful for the health of human beings and environment [12]. The use of inhibitors proves to be a good way to solve this problem [13-17]. Recent research indicated that metal complexes had interesting activities on urease [18-20]. However, the study on this topic is limited, and no definite relationship between structures and properties is given. Schiff

Heilongjiang Province Qiqihar Ecological Environment Monitoring Center, Qiqihar, People′s Republic of China; **qqhrwangyuan@163.com. Original article submitted May 16, 2021; revised June 4, 2021; accepted June 5, 2021.

* Supplementary materials are available for this article at doi 10.1134/S0022476621110020 and are accessible for authorized users.

bases are a kind of interesting ligands in the formation of metal complexes, which have received particular attention due to their facile synthesis, versatile structures, and good biological activities [21-24]. Schiff base complexes of copper and nickel are reported to have urease inhibitory activities [25-27]. In pursuit of exploring novel urease inhibitors, three new copper and nickel complexes $[Cu_2L_2(\mu_{1,1}\text{-}N_3)_2]$ (**1**), $[Cu(HL)_2]Br_2$ (**2**), and $[Ni_3L_2(DMF)_2(\mu_2\text{–}\eta^1\text{:}\eta^1\text{-}CH_3COO)_2(\mu_{1,1}\text{-}N_3)_2]$ (**3**), where L = 5-bromo-2-(((2-isopropylamino)ethyl)imino)methyl)phenolate, HL = 5-bromo-2-(((2-isopropylammonio)ethyl)imino) methyl)phenolate, are presented.

EXPERIMENTAL

General methods and materials. 4-Bromosalicylaldehyde and *N*-isopropylethane-1,2-diamine were purchased (Lancaster) and used as received. All other reagents were of analytical grade. The C, H, and N elemental analyses were carried out in a 2400 Series-II CHN analyzer. FTIR spectra were obtained on a Jasco FT/IR-4000 spectrometer with samples prepared as KBr pellets. Electronic spectra were obtained with a LAMBDA 35 spectrophotometer. Single crystal X-ray diffraction was carried out with a Bruker Apex II CCD diffractometer. Molar conductance was measured with a Shanghai DDS-11A conductometer.

Caution! Although our samples never exploded during handling, azide compounds are potentially explosive. Only a small amount of an azide compound should be prepared and it should be handled with care.

Synthesis of complex 1. 4-Bromosalicylaldehyde (0.20 g, 1.0 mmol) and *N*-isopropylethane-1,2-diamine (0.10 g, 1.0 mmol) were dissolved and mixed in methanol (30 mL). The mixture was stirred at room temperature for 10 min to give a yellow solution. A methanol solution (20 mL) containing copper bromide (0.22 g, 1.0 mmol) and sodium azide (0.065 g, 1.0 mmol) was added dropwise to the former solution The color immediately changed to blue. The mixture was further stirred at room temperature for 30 min and filtered. The filtrate was kept at ambient temperature. Single crystals of the complex, suitable for X-ray diffraction, were grown from the filtrate upon slow evaporation within a few days. The crystals were isolated by filtration, washed with methanol, and dried in air. Yield: 0.27 g (69%). Anal. calcd for $C_{12}H_{16}BrCuN_5O$ (%): C 36.98, H 4.14, N 17.97. Found (%): C 37.21, H 4.22, N 17.86. IR data (KBr, cm^{-1}): 3237, 2046, 1638, 1583, 1515, 1468, 1455, 1425, 1388, 1367, 1333, 1290, 1201, 1188, 1133, 1062, 988, 933, 917, 862, 783, 732, 621, 602, 536, 506, 463, 447. UV-Vis data in methanol (λ_{max} (nm), ε ($L \cdot mol^{-1} \cdot cm^{-1}$)): 230, 17230; 248, 16010; 272, 14633; 362, 7025.

Synthesis of complex 2. 4-Bromosalicylaldehyde (0.20 g, 1.0 mmol) and *N*-isopropylethane-1,2-diamine (0.10 g, 1.0 mmol) were dissolved and mixed in methanol (30 mL). The mixture was stirred at room temperature for 10 min to give a yellow solution. The solution was added dropwise with a methanol solution (20 mL) containing copper bromide (0.22 g, 1.0 mmol). The color immediately changed to blue. The mixture was further stirred at room temperature for 30 min and filtered. The filtrate was kept at ambient temperature. Single crystals of the complex, suitable for X-ray diffraction, were grown from the filtrate upon slow evaporation within a few days. The crystals were isolated by filtration, washed with methanol, and dried in air. Yield: 0.16 g (52%). Anal. calcd for $C_{24}H_{34}Br_4CuN_4O_2$ (%): C 36.32, H 4.32, N 7.06. Found (%): C 36.45, H 4.37, N 6.95. IR data (KBr, cm^{-1}): 3215, 1625, 1583, 1519, 1467, 1425, 1410, 1393, 1333, 1299, 1278, 1254, 1201, 1156, 1130, 1071, 1037, 999, 930, 915, 885, 854, 781, 740, 675, 621, 602, 542, 455, 412. UV-Vis data in methanol (λ_{max} (nm), ε ($L \cdot mol^{-1} \cdot cm^{-1}$)): 225, 18350; 250, 15670; 270, 13245; 364, 4710.

Synthesis of complex 3. 4-Bromosalicylaldehyde (0.20 g, 1.0 mmol) and *N*-isopropylethane-1,2-diamine (0.10 g, 1.0 mmol) were dissolved and mixed in methanol (30 mL). The mixture was stirred at room temperature for 10 min to give a yellow solution. The solution was added dropwise with a methanol solution (20 mL) containing nickel acetate tetrahydrate (0.25 g, 1.0 mmol). The color immediately changed to green. Then a few drops of DMF were added, and the mixture was further stirred at room temperature for 30 min and filtered. The filtrate was kept at ambient temperature. Single crystals of the complex, suitable for X-ray diffraction, were grown from the filtrate upon slow evaporation within a few days. The crystals were isolated by filtration, washed with methanol, and dried in air. Yield: 0.15 g (41%). Anal. calcd for $C_{34}H_{52}Br_2N_{12}Ni_3O_8$ (%): C 37.37, H 4.80, N 15.38. Found (%): C 37.23, H 4.87, N 15.26. IR data (KBr, cm^{-1}): 3271, 2068, 1656, 1585, 1572,

1525, 1427, 1395, 1342, 1290, 1254, 1205, 1190, 1133, 1105, 1073, 996, 979, 968, 925, 911, 864, 804, 785, 730, 672, 615, 600, 575, 467, 431. UV-Vis data in methanol (λ_{max} (nm), ε ($L \cdot mol^{-1} \cdot cm^{-1}$)): 228, 16380; 246, 16870; 307, 5127; 358, 2623; 408, 1712.

X-ray structure determination. Single crystal X-ray diffraction data for the complexes were collected on a Bruker Apex II CCD diffractometer at 298(2) K with MoK_α radiation (λ = 0.71073 Å) by the ω scan mode. The SAINT program was used for the integration of the diffraction profiles [28]. The structures were solved by direct methods using the SHELXS program of the SHELXTL package and refined by full-matrix least-squares methods with SHELXL (semi-empirical absorption corrections were applied using the SADABS program) [29, 30]. The positions of the non-hydrogen atoms were located in difference Fourier maps and least-squares refinement cycles, and finally refined anisotropically. All hydrogen atoms of the complexes were placed theoretically onto the specific atoms and refined isotropically as riding atoms. Crystallographic data and experimental details for structural analyses are summarized in Table 1. Selected bond lengths and angles for the complex are listed in Table 2.

Measurement of the urease inhibitory activity. The assay mixture, containing 25 μL (10U) of jack bean urease which was replaced by 25 μL of a cell suspension (4.0×10^7 CFU/mL) for the urease assay of intact cells and 25 μL of the test compound, was pre-incubated for 1.5 h at room temperature in a 96-well assay plate. The urease activity was determined by measuring the ammonia production using the indophenol method as described by Weatherburn [31].

TABLE 1. Crystallographic Data and Refinement Details for the Complexes

Parameter	**1**	**2**	**3**
Formula	$C_{12}H_{16}BrCuN_5O$	$C_{24}H_{34}Br_4CuN_4O_2$	$C_{34}H_{52}Br_2N_{12}Ni_3O_8$
Formula weight	389.75	793.73	1092.83
Crystal color, shape	Blue, block	Blue, block	Green, block
Crystal system	Monoclinic	Monoclinic	Triclinic
Space group	$P2_1/n$	$C2/c$	$P\bar{1}$
a, *b*, *c*, Å	9.6582(12), 14.9942(12), 10.7013(11)	22.6497(13), 21.8313(10), 15.2635(12)	9.8456(13), 11.4288(11), 11.4800(13)
α, β, γ, deg	90, 109.207(1), 90	90, 129.232(1), 90	109.496(2), 98.384(2), 95.295(2)
V, Å^3	1463.5(3)	5846.1(6)	1190.9(2)
Z	4	8	1
D_{calcd}, g/cm^3	1.769	1.804	1.524
M, MoK_α, mm^{-1}	4.225	6.243	2.908
θ range collection, deg	2.43–25.50	1.49–25.50	1.91–25.50
Min. / max. transmission	0.5007 / 0.5168	0.2937 / 0.3277	0.5671 / 0.6377
Reflections collected	7632	15472	6213
Unique	2723	5437	4372
Observed reflections ($I \geq 2\sigma(I)$)	2230	3544	3007
Data/restraints/parameters	2723/0/183	5437/0/323	4372/0/273
Goodness of fit on F^2	1.025	1.084	1.028
R_1, wR_2 ($I \geq 2\sigma(I)$) / (all data)[a]	0.0364, 0.0893 / 0.0485, 0.0951	0.0495, 0.1309 / 0.0913, 0.1499	0.0641, 0.1690 / 0.0957, 0.1953

[a] $R_1 = F_0 - F_c/F_0$, $wR_2 = \{\sum w(F_0^2 - F_c^2)^2 / \sum w(F_0^2)^2\}^{1/2}$.

TABLE 2. Selected Bond Distances (Å) and Angles (deg) of the Complexes

1			
Cu1–O1	1.918(3)	Cu1–N1	1.942(3)
Cu1–N2	2.071(3)	Cu1–N3	1.985(3)
Cu1–N3A	2.459(3)		
O1–Cu1–N1	93.08(12)	O1–Cu1–N3	89.63(12)
N1–Cu1–N3	173.79(14)	O1–Cu1–N2	176.10(12)
N1–Cu1–N2	84.35(13)	N3–Cu1–N2	92.64(12)
O1–Cu1–N3$^{\#1}$	95.04(11)	N1–Cu1–N3$^{\#1}$	97.19(13)
N3–Cu1–N3$^{\#1}$	88.13(12)	N2–Cu1–N3$^{\#1}$	88.21(12)
Symmetry code: $^{\#1}$ 1–*x*, 1–*y*, 1–*z*.			
2			
Cu1–O1	1.927(5)	Cu1–N1	2.020(6)
O1–Cu1–O1$^{\#1}$	180	O1–Cu1–N1	91.3(2)
O1–Cu1–N1$^{\#1}$	88.7(2)	N1–Cu1–N1$^{\#1}$	180
Cu2–O2	1.912(5)	Cu2–N3	2.021(6)
O2–Cu2–O2$^{\#2}$	180	O2–Cu2–N3$^{\#2}$	89.0(2)
O2–Cu2–N3	91.0(2)	N3–Cu2–N3$^{\#2}$	180
Symmetry codes: $^{\#1}$1–*x*, 1–*y*, 1–*z*; $^{\#2}$ 3/2–*x*, 3/–*y*, 1–*z*.			
3			
Ni1–N1	2.031(5)	Ni1–O1	2.033(4)
Ni1–O2	2.067(4)	Ni1–N3	2.107(5)
Ni1–O4	2.124(5)	Ni1–N2	2.152(5)
Ni2–O3	2.061(4)	Ni2–O1	2.067(4)
Ni2–N3	2.120(5)		
N1–Ni1–O1	88.00(17)	N1–Ni1–O2	92.84(18)
O1–Ni1–O2	93.60(16)	N1–Ni1–N3	170.07(19)
O1–Ni1–N3	82.28(17)	O2–Ni1–N3	89.83(18)
N1–Ni1–O4	86.73(19)	O1–Ni1–O4	92.23(18)
O2–Ni1–O4	174.14(17)	N3–Ni1–O4	91.59(19)
N1–Ni1–N2	82.39(19)	O1–Ni1–N2	169.90(17)
O2–Ni1–N2	83.80(18)	N3–Ni1–N2	107.42(19)
O4–Ni1–N2	90.35(19)	O3–Ni2–O3$^{\#1}$	180
O3–Ni2–O1$^{\#1}$	90.77(16)	O3–Ni2–O1	89.23(16)
O3–Ni2–O1$^{\#1}$	90.77(16)	O1–Ni2–O1$^{\#1}$	180
O3–Ni2–N3$^{\#1}$	89.38(18)	O1–Ni2–N3$^{\#1}$	98.85(17)
O3–Ni2–N3	90.62(18)	O1–Ni2–N3	81.15(17)
N3–Ni2–N3$^{\#1}$	180		
Symmetry code: $^{\#1}$ 1–*x*, 1–*y*, 1–*z*.			

RESULTS AND DISCUSSION

General chemistry. The Schiff base ligand was prepared by the reaction of 4-bromosalicylaldehyde and *N*-isopropylethane-1,2-diamine in methanol. The ligand was not isolated and purified, and was used to prepare complexes with copper and nickel salts. Elemental analyses of the complexes are in accordance with the molecular structures proposed by the X-ray analysis. The complexes are stable in air at room temperature. The molar conductivity of complexes **1** and **3** measured in methanol at concentration of 10^{-3} mol/L is 15-37 $\Omega^{-1}\cdot cm^2/mol$, indicating their non-electrolytic nature in the solution [32]. However, the molar conductivity of complex **2** is 205 $\Omega^{-1}\cdot cm^2/mol$, indicating it is a 1:2 electrolyte in the solution [32].

IR and UV-vis spectra. In the IR spectra, weak and sharp absorption bands in the range of 3215-3271 cm^{-1} are assigned to the N–H vibrations of the Schiff base ligands. The characteristic C=N stretching is observed at 1625-1656 cm^{-1} as intense signals [33]. The ν_{asym}(COO) and ν_{sym}(COO) vibrations of the acetate ligands in complex **3** are observed at 1572 cm^{-1} and 1427 cm^{-1}, respectively. The difference between the two bands ($\Delta\nu$ = 145 cm^{-1}) is smaller than 164 cm^{-1} observed in ionic acetate, indicating the bidentate bridging coordination mode [34, 35]. The IR spectra of complexes **1** and **3** show strong bands at 2046-2068 cm^{-1} characteristic of the azide ligands [36, 37]. The Ar–O stretching bands are located at 1156-1190 cm^{-1} [38].

In the UV-Vis spectra, the bands at 225-250 nm and 270-307 nm are attributed to the π–π* and *n*–π* transitions [39]. The bands at 358-408 nm can be assigned to the ligand-to-metal charge transition (LMCT) [40].

Structural description of complex 1. The molecular structure of the end-on azido-bridged dinuclear copper complex is shown in Fig. 1. The molecule possesses the crystallographic inversion center of symmetry. The Cu atoms are bridged by two azide ligand, with a distance of 3.210(1) Å. The Cu atom is coordinated in a square pyramidal geometry, with the basal plane being defined by phenolate oxygen atoms, imino and amino nitrogen atoms of the Schiff base ligand, and one azide N atom, with the apical position being occupied by another azide N atom. The Cu atom deviates from the basal plane by 0.074(2) Å. The square pyramidal coordination is distorted from the ideal model, as evidenced by the bond angles. The *cis* and *trans* angles in the basal plane are in the ranges of 84.35(13)-93.08(12)° and 173.79(14)-176.10(12)°, respectively. The bond angles among the apical and basal donor atoms are in the range of 88.13(12) -97.19(13)°. The Cu–O and Cu–N bond lengths are comparable to those observed in Schiff base copper complexes with azide ligands [41, 42].

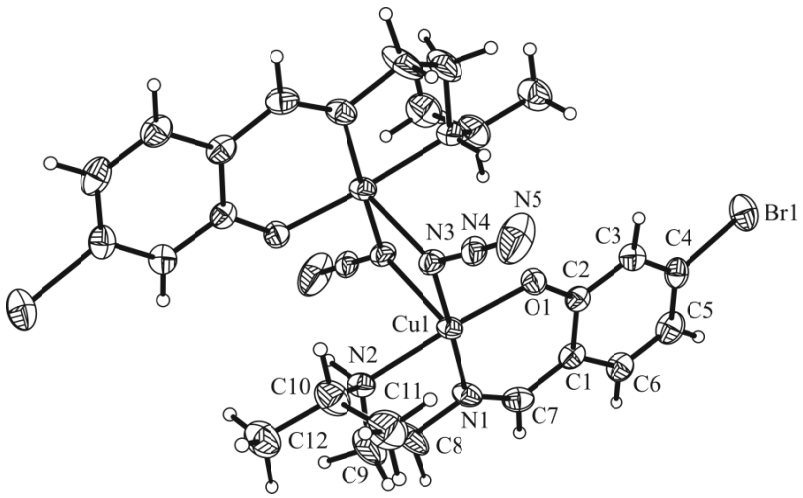

Fig. 1. A perspective view of the molecular structure of complex **1**. Thermal ellipsoids are drawn at the 30% probability level. Unlabeled atoms are related to the symmetry operation 1–*x*, 1–*y*, 1–*z*.

In the crystal structure of the complex, the molecules are stacked along the *a* axis *via* π···π interactions (*Cg*1···*Cg*2$^{\#1}$ 4.484(5) Å, *Cg*2···*Cg*2$^{\#1}$ 3.820(5) Å, symmetry code: $^{\#1}$ 1–*x*, 1–*y*, –*z*; *Cg*1 and *Cg*2 are the centroids of Cu1–O1–C2–C1–C7–N1 and C1–C2–C3–C4–C5–C6, respectively) (Fig. 2).

Structural description of complex 2. The molecular structure of complex **2** is shown in Fig. 3. The asymmetric unit of the complex contains two $[Cu(HL)_2]^{2+}$ cations and four bromide anions. The molecules possess crystallographic inversion centers of symmetry. The Cu atom in each cation is coordinated by two phenolate oxygen atoms and two imino nitrogen atoms from two Schiff base ligands, forming a square planar geometry. The amino nitrogen atom is protonated, and does not participate in coordination. The Cu–O and Cu–N bond lengths are comparable to those observed in Schiff base copper complexes [38, 39].

As shown in Fig. 4, the complex cations and the bromide anions are linked through N–H···O, N–H···Br, C–H···O, and C–H···Br hydrogen bonds (Table 3), to form a network. In addition, there are π···π interactions (*Cg*3···*Cg*3$^{\#3}$ 3.840(5) Å, *Cg*4···*Cg*4$^{\#4}$ 4.403(5) Å, symmetry codes: $^{\#3}$ –*x*, *y*, 1/2–*z*; $^{\#4}$ 1–*x*, *y*, 3/2–*z*; *Cg*3 and *Cg*4 are the centroids of C1–C2–C3–C4–C5–C6 and C13–C14–C15–C16–C17–C18, respectively) among the molecules.

Structural description of complex 3. The molecular structure of phenolate, azide, and acetate bridged complex **3** is shown in Fig. 5. The molecule possesses the crystallographic inversion center of symmetry. The Ni···Ni distance is 3.069(1) Å. The outer Ni atom is coordinated in the octahedral geometry, with the equatorial plane being defined by the phenolate oxygen atom, imino and amino nitrogen atoms of the Schiff base ligand, and one terminal N atom of the end-on azide ligand. The axial positions are occupied by one O atom of the μ_2–η^1:η^1-acetate ligand and one O atom of the DMF ligand. The Ni atom deviates from the equatorial plane by 0.011(2) Å. The octahedral coordination is distorted from the ideal model, as evidenced by the bond angles. The *cis* and *trans* angles in the equatorial plane are in the ranges of 82.28(17)-107.42(19)° and 169.90(17)-170.07(19)°, respectively. The bond angles among the axial and equatorial donor atoms are in the ranges of 83.80(18)-93.60(16)°. The inner Ni atom is coordinated in the octahedral geometry. The equatorial plane is defined by two phenolate oxygen from two Schiff base ligands, and two N atoms from two azide ligands. The axial positions are occupied by two O atoms from two acetate ligands. The octahedral coordination is distorted from ideal model, as evidenced by the bond angles. The *cis* angles in the equatorial plane are in the range of 81.15(17)-98.85(17)°. The bond angles among the axial and equatorial donor atoms are in the range of 89.38(18)-90.77(16)°. The Ni–O and Ni–N bond lengths are comparable to those observed in Schiff base nickel complexes with acetate and azide ligands [40, 41].

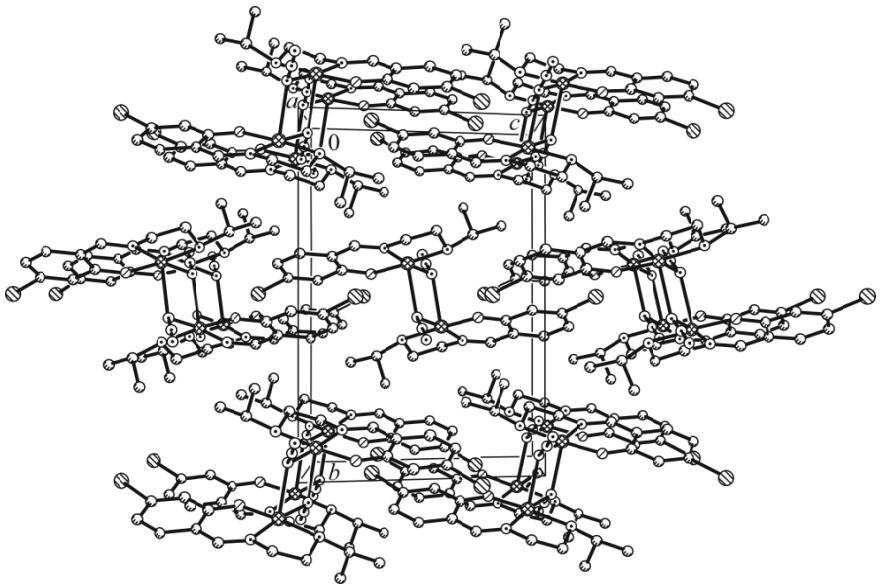

Fig. 2. Molecular packing structure of complex **1**. Hydrogen bonds are drawn as dashed lines.

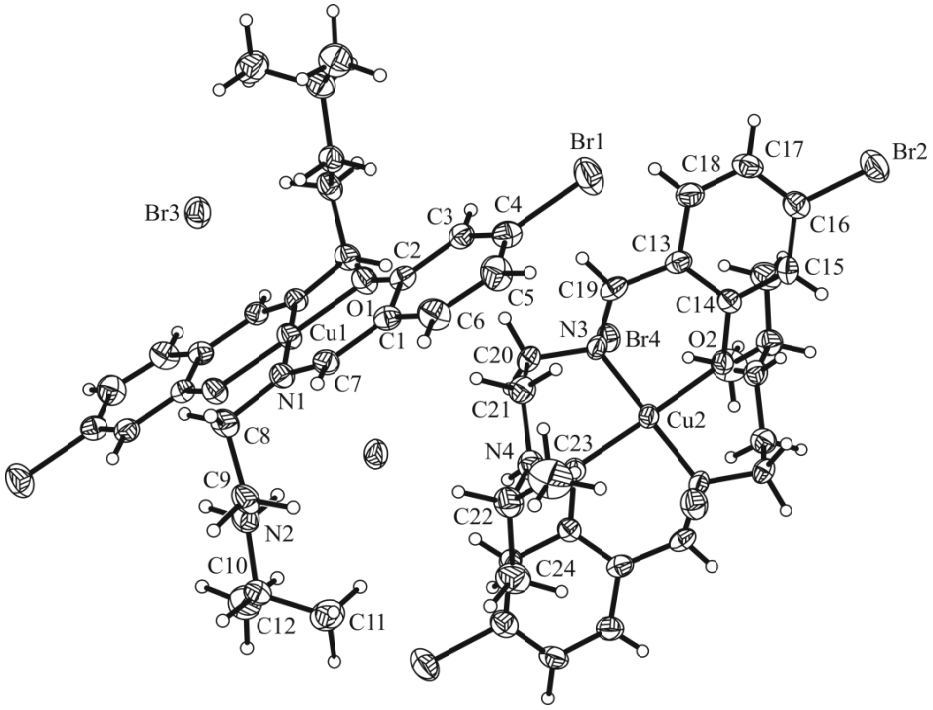

Fig. 3. A perspective view of the molecular structure of complex **2**. Thermal ellipsoids are drawn at the 30% probability level. Unlabeled atoms are related to the symmetry operations 1–*x*, 1–*y*, 1–*z* and 3/2–*x*, 3/–*y*, 1–*z*.

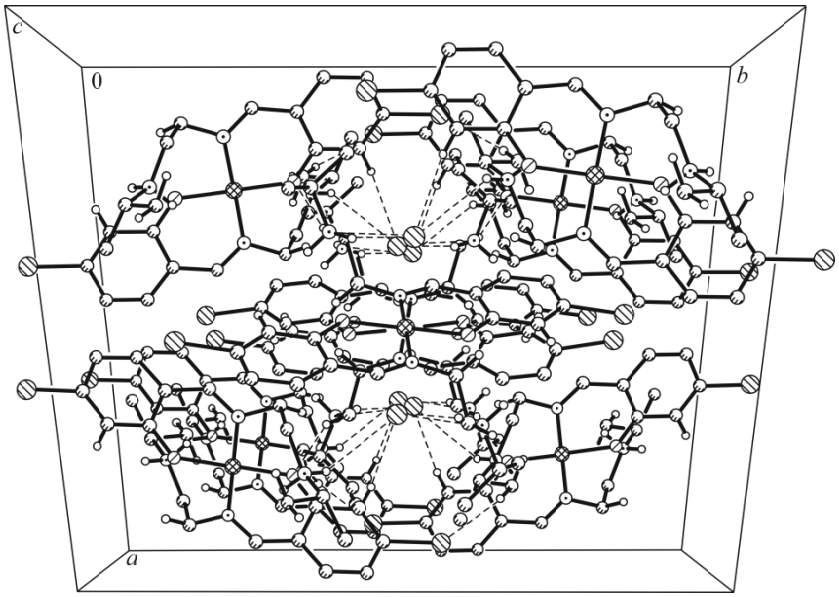

Fig. 4. Molecular packing structure of complex **2**. Hydrogen bonds are drawn as dashed lines.

As shown in Fig. 6, the complex molecules of complex **3** are linked through N–H···Br hydrogen bonds, to form chains along the *b* axis. In addition, there are π···π interactions among the molecules (*Cg*5···*Cg*5$^{\#5}$ 4.690(5) Å, symmetry code: $^{\#5}$ –*x*, 1–*y*, 1–*z*; *Cg*5 is the centroid of C1–C2–C3–C4–C5–C6).

Urease inhibitory activity. We investigated the urease inhibition of the three complexes in an effort to find more potent compounds in comparison with the previously reported compounds. The IC_{50} values of complexes **1** and **2** are

TABLE 3. Hydrogen Bond Distances (Å) and Bond Angles (deg) of the Complexes

D–H···*A*	*d*(*D*–H)	*d*(H···*A*)	*d*(*D*···*A*)	Angle (*D*–H···*A*)
		2		
N2–H2A···O1$^{\#1}$	0.90	2.54	2.862(5)	102(6)
N2–H2A···Br3$^{\#2}$	0.90	2.47	3.352(5)	168(6)
N2–H2B···Br4	0.90	2.76	3.374(5)	126(6)
N2–H2B···O1$^{\#1}$	0.90	2.45	2.862(5)	109(6)
N4–H4A···Br4	0.90	2.44	3.328(5)	168(6)
N4–H4A···O2$^{\#3}$	0.90	2.58	2.888(5)	101(6)
N4–H4B···Br3$^{\#3}$	0.90	2.82	3.451(5)	128(6)
N4–H4B···O2$^{\#3}$	0.90	2.47	2.888(5)	109(6)
C3–H3···Br4$^{\#1}$	0.93	2.90	3.826(5)	176(6)
C8–H8A···O1$^{\#1}$	0.97	2.33	2.854(5)	113(6)
C9–H9B···O2	0.97	2.44	3.341(5)	155(6)
C15–H15···Br3	0.93	2.93	3.850(5)	172(6)
C20–H20A···O2$^{\#3}$	0.97	2.30	2.840(5)	114(6)
C23–H23B···Br2$^{\#4}$	0.96	2.91	3.819(5)	160(6)
		3		
N2–H2···Br1$^{\#5}$	0.91	2.86	3.761(4)	171(5)
C11–H11C···O4	0.96	2.57	3.214(4)	125(5)
C15–H15···O3$^{\#6}$	0.93	2.53	3.454(4)	171(5)

Symmetry codes: $^{\#1}$ –*x*, –*y*, –*z*; $^{\#2}$ *x*, –*y*, –1/2+*z*; $^{\#3}$ 1/2–*x*, 1/2–*y*, 1–*z*; $^{\#4}$ 1/2–*x*, 1/2+*y*, 1/2–*z*; $^{\#5}$ *x*, –1+*y*, *z*; $^{\#6}$ 1–*x*, 1–*y*, 1–*z*.

1.23±0.12 μmol/L and 0.87±0.09 μmol/L, respectively. However, complex **3** has a weak activity, with the IC_{50} value of 31.3±1.85 μmol/L. Thus, it is obvious that copper complexes have more potent urease inhibition than nickel complexes. This trend is in accordance with those reported in the literature [42-46]. Moreover, the nickel complex is larger than the copper

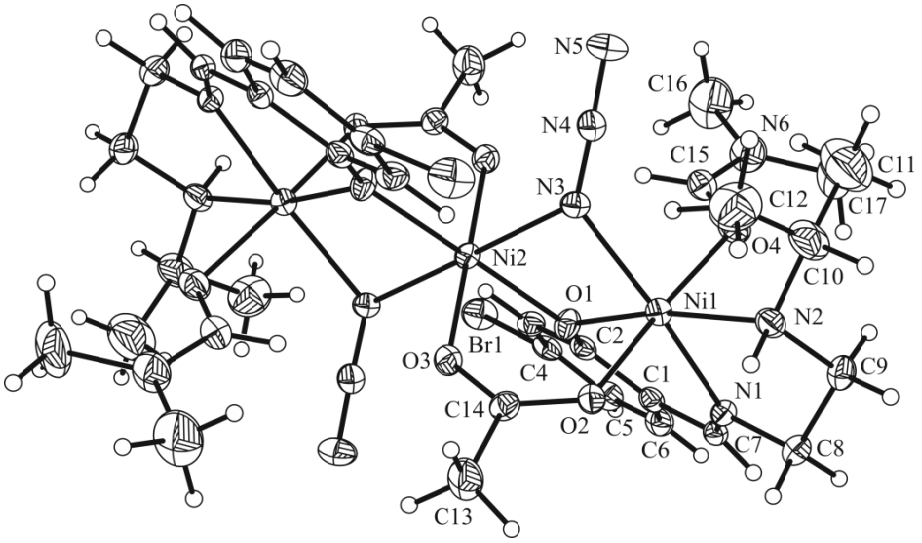

Fig. 5. A perspective view of the molecular structure of complex **3**. Thermal ellipsoids are drawn at the 30% probability level. Unlabeled atoms are related to the symmetry operation 1–*x*, 1–*y*, 1–*z*.

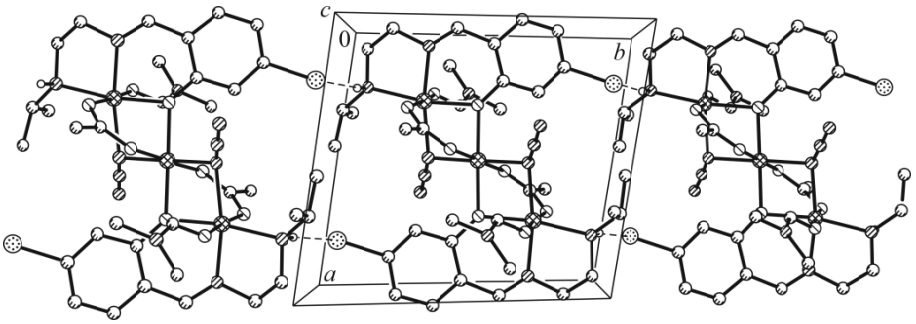

Fig. 6. Molecular packing structure of complex **3**. Hydrogen bonds are drawn as dashed lines.

complexes, illustrating that the hydrophobic area of the enzyme cannot comfortably accommodate the large molecule. From the comparison of these copper complexes with Schiff base copper complexes found in the literature, it can be seen that when a bromine atom was introduced to the Schiff base ligand, the resulting complexes had increased activities. Acetohydroxamic acid and copper perchlorate were used as references, with IC_{50} values of 27.8±2.12 μmol/L and 9.1±1.5 μmol/L, respectively. The urease inhibition of copper perchlorate is weaker than that of the copper complexes. Thus, the two copper complexes would be potential urease inhibitors that deserve further study.

CONCLUSIONS

Aiming at obtaining new and efficient urease inhibitors, three new copper and nickel complexes with Schiff base ligands have been synthesized and characterized. Single crystal structures of the complexes were confirmed by X-ray diffraction and described. The copper complexes have a strong urease inhibitory activity, which deserves further study to explore novel and efficient urease inhibitors.

Supplementary materials. X-ray crystallographic data for the complexes have been deposited with the Cambridge Crystallographic Data Centre (The Director, CCDC, 12 Union Road, Cambridge, CB2 1 EZ, UK; e-mail: deposit@ccdc.cam.ac.uk; http://www.ccdc.cam.ac.uk; fax: +44-(0)1223–336033) and are available free of charge on request, quoting the deposition numbers CCDC 2062918-2062920.

ACKNOWLEDGMENTS

This project was supported by the Heilongjiang Province Qiqihar Ecological Environment Monitoring Center.

CONFLICT OF INTERESTS

The author declares that he has no conflict of interests.

REFERENCES

1. L. Casali, L. Mazzei, O. Shemchuk, L. Sharma, K. Honer, F. Grepioni, S. Ciurli, D. Braga, and J. Baltrusaitis. *ACS Sustainable Chem. Eng.*, **2019**, *7*, 2852-2859. https://doi.org/10.1021/acssuschemeng.8b06293
2. P. A. Karplus, M. A. Pearson, and R. P. Hausinger. *Acc. Chem. Res.*, **1997**, *30*, 330-337. https://doi.org/10.1021/ar960022j
3. B. Bano, Kanwal, K. M. Khan, A. Lodhi, U. Salar, F. Begum, M. Ali, M. Taha, and S. Perveen. *Bioorg. Chem.*, **2018**, *80*, 129-144. https://doi.org/10.1016/j.bioorg.2018.06.007

4. P. Y. Oikawa, C. Ge, J. Wang, J. R. Eberwein, L. L. Liang, L. A. Allsman, D. A. Grantz, and G. D. Jenerette. *Nat. Commun.*, **2015**, *6*, 8753. https://doi.org/10.1038/ncomms9753
5. D. Coskun, D. T. Britto, W. Shi, and H. J. Kronzucker. *Nat. Plants*, **2017**, *3*, 17074. https://doi.org/10.1038/nplants.2017.74
6. S. V. Krupa. *Environ. Pollut.*, **2003**, *124*, 179-221. https://doi.org/10.1016/S0269-7491(02)00434-7
7. J. L. Hand, B. A. Schichtel, M. Pitchford, W. C. Malm, and N. H. Frank. *J. Geophys. Res. Atmos.*, **2012**, *117*, D05209. https://doi.org/10.1029/2011JD017122
8. J. N. Galloway, F. J. Dentener, D. G. Capone, E. W. Boyer, R. W. Howarth, S. P. Seitzinger, G. P. Asner, C. C. Cleveland, P. A. Green, E. A. Holland, D. M. Karl, A. F. Michaels, J. H. Porter, A. R. Townsend, and C. J. Vorosmarty. *Biogeochemistry*, **2004**, *70*, 153-226. https://doi.org/10.1007/s10533-004-0370-0
9. Z.-P. Xiao, Z.-Y. Peng, J.-J. Dong, J. He, H. Ouyang, Y.-T. Peng, C.-L. Lu, W.-Q. Lin, J.-X. Wang, Y.-P. Xiang, and H.-L. Zhu. *Eur. J. Med. Chem.*, **2013**, *63*, 685-695. https://doi.org/10.1016/j.ejmech.2013.03.016
10. A. Hameed, K. M. Khan, S. T. Zehra, R. Ahmed, Z. Shafiq, S. M. Bakht, M. Yaqub, M. Hussain, A. de la Vega de Leon, N. Furtmann, J. Bajorath, H. A. Shad, M. N. Tahir, and J. Iqbal. *Bioorg. Chem.*, **2015**, *61*, 51-57. https://doi.org/10.1016/j.bioorg.2015.06.004
11. F. Iftikhar, Y. Ali, F. A. Kiani, S. F. Hassan, T. Fatima, A. Khan, B. Niaz, A. Hassan, F. L. Ansari, and U. Rashid. *Bioorg. Chem.*, **2017**, *74*, 53-65. https://doi.org/10.1016/j.bioorg.2017.07.003
12. W.-W. Ni, Q. Liu, S.-Z. Ren, W.-Y. Li, L.-L. Yi, H. Jing, L.-X. Sheng, Q. Wan, P.-F. Zhong, H.-L. Fang, H. Ouyang, Z.-P. Xiao, and H.-L. *Zhu. Bioorg. Med. Chem.*, **2018**, *26*, 4145-4152. https://doi.org/10.1016/j.bmc.2018.07.003
13. Q. Liu, W.-K. Shi, S.-Z. Ren, W.-W. Ni, W.-Y. Li, H.-M. Chen, P. Liu, J. Yuan, X.-S. He, J.-J. Liu, P. Cao, P.-Z. Yang, Z.-P. Xiao, and H.-L. Zhu. *Eur. J. Med. Chem.*, **2018**, *156*, 126-136. https://doi.org/10.1016/j.ejmech.2018.06.065
14. W.-W. Ni, H.-L. Fang, Y.-X. Ye, W.-Y. Li, C.-P. Yuan, D.-D. Li, S.-J. Mao, S.-E. Li, Q.-H. Zhu, H. Ouyang, Z.-P. Xiao, and H.-L. Zhu. *Future Med. Chem.*, **2020**, *12*, 1633-1645. https://doi.org/10.4155/fmc-2020-0048
15. W.-K. Shi, R.-C. Deng, P.-F. Wang, Q.-Q. Yue, Q. Liu, K.-L. Ding, M.-H. Yang, H.-Y. Zhang, S.-H. Gong, M. Deng, W.-R. Liu, Q.-J. Feng, Z.-P. Xiao, and H.-L. Zhu. *Bioorg. Med. Chem.*, **2016**, *24*, 4519-4527. https://doi.org/10.1016/j.bmc.2016.07.052
16. Z.-P. Xiao, W.-K. Shi, P.-F. Wang, W. Wei, X.-T. Zeng, J.-R. Zhang, N. Zhu, M. Peng, B. Peng, X.-Y. Lin, H. Ouyang, X.-C. Peng, G.-C. Wang, and H.-L. Zhu. *Bioorg. Med. Chem.*, **2015**, *23*, 4508-4513. https://doi.org/10.1016/j.bmc.2015.06.014
17. Z.-P. Xiao, Z.-Y. Peng, J.-J. Dong, R.-C. Deng, X.-D. Wang, H. Ouyang, P. Yang, J. He, Y.-F. Wang, M. Zhu, X.-C. Peng, W.-X. Peng, and H.-L. Zhu. *Eur. J. Med. Chem.*, **2013**, *68*, 212-221. https://doi.org/10.1016/j.ejmech.2013.07.047
18. M. K. Rauf, S. Yaseen, A. Badshah, S. Zaib, R. Arshad, Imtiaz-ud-Din, M. N. Tahir, and J. Iqbal. *J. Biol. Inorg. Chem.*, **2015**, *20*, 541-554. https://doi.org/10.1007/s00775-015-1239-5
19. X. Dong, Y. Li, Z. Li, Y. Cui, and H. Zhu. *J. Inorg. Biochem.*, **2012**, *108*, 22-29. https://doi.org/10.1016/j.jinorgbio.2011.12.006
20. Y. Gou, M. Yu, Y. Li, Y. Peng, and W. Chen. *Inorg. Chim. Acta*, **2013**, *404*, 224-229. https://doi.org/10.1016/j.ica.2013.03.045
21. S. Najm, H. Naureen, K. Sultana, F. Anwar, M. M. Khan, H. Nadeem, and M. Saeed. *ACS Omega*, **2021**, *6*, 7719-7730. https://doi.org/10.1021/acsomega.1c00027
22. T. Chandrasekar, A. Arunadevi, and N. Raman. *J. Coord. Chem.*, **2021**, *74*, 804-822. https://doi.org/10.1080/00958972.2020.1870967

23. A. Arunadevi and N. Raman. *J. Coord. Chem.*, **2020**, *73*, 2095-2116. https://doi.org/10.1080/00958972.2020.1824293
24. C. J. Dhanaraj and S. S. S. Raj. *Inorg. Chem. Commun.*, **2020**, *119*, 108087. https://doi.org/10.1016/j.inoche.2020.108087
25. H. Zhu, Z.-Z. Wang, B. Qi, T. Huang, and H.-L. Zhu. *J. Coord. Chem.*, **2013**, *66*, 2980-2991. https://doi.org/10.1080/00958972.2013.821198
26. L. Habala, A. Roller, M. Matuska, J. Valentova, A. Rompel, and F. Devinsky. *Inorg. Chim. Acta*, **2014**, *421*, 423-426. https://doi.org/10.1016/j.ica.2014.06.035
27. Y.-G. Li, D.-H. Shi, H.-L. Zhu, H. Yan, and S. W. Ng. *Inorg. Chim. Acta*, **2007**, *360*, 2881-2889. https://doi.org/10.1016/j.ica.2007.02.019
28. G. M. Sheldrick. SAINT (version 6.02), SADABS (version 2.03). Madison, WI, USA: Bruker AXS, **2002**.
29. G. M. Sheldrick. *Acta Crystallogr*., *Sect. C*, **2015**, *71*, 3-8. https://doi.org/10.1107/S2053229614024218
30. G. M. Sheldrick. SADABS Program for Empirical Absorption Correction of Area Detector. Gottingen, Germany: University of Gottingen, **1996**.
31. M. W. Weatherburn. *Anal. Chem.*, **1967**, *39*, 971-974. https://doi.org/10.1021/ac60252a045
32. W. J. Geary. *Coord. Chem. Rev.*, **1971**, *7*, 81-122. https://doi.org/10.1016/S0010-8545(00)80009-0
33. K. R. Surati and B. T. Thaker. *Spectrochim. Acta*, *Part A*, **2010**, *75*, 235-242. https://doi.org/10.1016/j.saa.2009.10.018
34. B. Sarkar, M. G. B. Drew, M. Estrader, C. Diaz, and A. Ghosh. *Polyhedron*, **2008**, *27*, 2625-2633. https://doi.org/10.1016/j.poly.2008.05.004
35. U. Kumar, J. Thomas, and N. Thirupathi. *Inorg. Chem.*, **2010**, *49*, 62-72. https://doi.org/10.1021/ic901100z
36. S. S. Massoud and F. A. Mautner. *Inorg. Chim. Acta*, **2005**, *358*, 3334-3340. https://doi.org/10.1016/j.ica.2005.05.007
37. A. Ray, S. Banerjee, R. J. Butcher, C. Desplanches, and S. Mitra. *Polyhedron*, **2008**, *27*, 2409-2415. https://doi.org/10.1016/j.poly.2008.04.018
38. Y.-M. Zhou, X.-R. Ye, F.-B. Xin, and X.-Q. Xin. *Transition Met. Chem.*, **1999**, *24*, 118-120. https://doi.org/10.1023/A:1006989707001
39. L. Pogany, J. Moncol, M. Gal, I. Salitros, and R. Boca. *Inorg. Chim. Acta*, **2017**, *462*, 23-29. https://doi.org/10.1016/j.ica.2017.03.001
40. A. Jayamani, M. Sethupathi, S. O. Ojwach, and N. Sengottuvelan. *Inorg. Chem. Commun.*, **2017**, *84*, 144-149. https://doi.org/10.1016/j.inoche.2017.08.013
41. P. K. Bhaumik, K. Harms, and S. Chattopadhyay. *Polyhedron*, **2014**, *68*, 346-356. https://doi.org/10.1016/j.poly.2013.10.031
42. J. Wang, Y. Luo, Y. Zhang, Y. Chen, F. Gao, Y. Ma, D. Xian, and Z. You. *J. Coord. Chem.*, **2021**, *74*, 1028-1038. https://doi.org/10.1080/00958972.2020.1861603
43. M. Duan, Y. Li, L. Xu, H. Yang, F. Luo, Y. Guan, B. Zhang, C. Jing, and Z. You. *Inorg. Chem. Commun.*, **2019**, *100*, 27-31. https://doi.org/10.1016/j.inoche.2018.12.009
44. Z. You, H. Yu, Z. Li, W. Zhai, Y. Jiang, A. Li, S. Guo, K. Li, C. Lv, and C. Zhang. *Inorg. Chim. Acta*, **2018**, *480*, 120-126. https://doi.org/10.1016/j.ica.2018.05.020
45. L. Pan, C. Wang, K. Yan, K. Zhao, G. Sheng, H. Zhu, X. Zhao, D. Qu, F. Niu, and Z. You. *J. Inorg. Biochem.*, **2016**, *159*, 22-28. https://doi.org/10.1016/j.jinorgbio.2016.02.017
46. Y. Luo, J. Wang, B. Zhang, Y. Guan, T. Yang, X. Li, L. Xu, J. Wang, and Z. You. *J. Coord. Chem.*, **2020**, *73*, 1765-1777. https://doi.org/10.1080/00958972.2020.1795645